Growth kinetics and formation mechanisms of complex organics by sequential reactions of acetylene with ionized aromatics

ARTICLE *in* INTERNATIONAL JOURNAL OF MASS SPECTROMETRY · AUGUST 2014

Impact Factor: 1.97 · DOI: 10.1016/j.ijms.2014.08.023

4 AUTHORS:

Abdel Rahman Soliman
Virginia Commonwealth University
13 PUBLICATIONS **61** CITATIONS
SEE PROFILE

Isaac Attah
Virginia Commonwealth University
14 PUBLICATIONS **25** CITATIONS
SEE PROFILE

Ahmed Hamid
Pacific Northwest National Laboratory
24 PUBLICATIONS **91** CITATIONS
SEE PROFILE

M. Samy El-Shall
Virginia Commonwealth University
272 PUBLICATIONS **4,514** CITATIONS
SEE PROFILE

International Journal of Mass Spectrometry 377 (2015) 139–151

Contents lists available at ScienceDirect

International Journal of Mass Spectrometry

journal homepage: www.elsevier.com/locate/ijms

Growth kinetics and formation mechanisms of complex organics by sequential reactions of acetylene with ionized aromatics

Abdel-Rahman Soliman, Isaac K. Attah, Ahmed M. Hamid, M. Samy El-Shall *

Department of Chemistry, Virginia Commonwealth University, Richmond, VA 23284-2006, USA

ARTICLE INFO

Article history:
Received 16 May 2014
Received in revised form 5 August 2014
Accepted 7 August 2014
Available online 19 August 2014

ABSTRACT

In this work, we present direct experimental evidence for the formation of covalently-bonded organic ions by gas phase reactions of acetylene with the benzonitrile, phenylacetylene, and styrene radical cations, and compare these results with the previously studied acetylene reactions with the benzene, phenyl, pyridine, and pyrimidine cations. A very wide range of reaction rates has been found ranging from very slow reactions with energy barriers as in the case of benzene and styrene radical cations to reactions occurring at the collision rate as in the case of the pyrimidinium cation. In all cases, synthetic channels with increased numbers of carbon atoms are found in all the observed reactions. The resulting covalently-bonded precursor ions can undergo further growth to form polycyclic aromatic hydrocarbon ions including nitrogen-containing PAH ions. The observed chemistry under a wide range of experimental conditions, including extreme temperatures as high as 650 K, strongly implies a series of ion–molecule reactions that can lead from a simple molecule such as acetylene to polycyclic complex organic ions. The product ions resulting from the sequential reactions of acetylene can, in turn be neutralized by charge transfer or recombination, to produce large neutral PAHs. Therefore, ion–molecule reactions can contribute to the formation of higher hydrocarbons and PAHs in ionizing environments. The observed reactions could explain the possible formation of complex organics under a wide range of temperatures and pressures in astrochemical environments such as the nitrogen-rich Titan's atmosphere.

1. Introduction

Formation mechanisms of complex organics in the gas phase play important roles in flames and combustion processes particularly for the mechanisms of soot formation and the generation of organic aerosols throughout the atmosphere as well as in interstellar clouds and solar nebula particularly for the origin of the observed complex organics [1–10]. These complex organics contain diverse molecules including acetylene, benzene, polycyclic aromatic hydrocarbons (PAHs), and polycyclic aromatic nitrogen heterocyclics (PANHs) [7–15].

Gas phase ion–molecule and cluster ion experiments are uniquely suited for the discovery of novel catalytic pathways that can lead to the formation of complex organics. These experiments can identify the chains of reactions leading to the formation of PAHs and PANHs found in soot, combustion, organic aerosols, interstellar clouds, and meteorites [16–27]. They can also provide detailed information on the reactivity, kinetics, growth mechanisms, energy barriers, and structures of large organic ions as well as on their complexes with associated solvent molecules in different environments [28–30].

Since acetylene is the smallest organic molecule that can be polymerized, extensive studies have been focused on the ion chemistry of acetylene clusters leading to the formation of cyclic covalent ions such as cyclobutadiene ($C_4H_4^{\bullet+}$) and benzene ($C_6H_6^{\bullet+}$) [31–41]. However, the most conclusive evidence for the efficient formation of the benzene radical cation following the electron impact (EI) ionization of large acetylene clusters was provided through a combination of mass-selected ion mobility and ion dissociation experiments coupled with theoretical calculations [36,37]. Accordingly, the collision cross section in helium and the fragmentation pattern of the $C_6H_6^{\bullet+}$ ion formed in ionized acetylene clusters are identical to those measured for the actual benzene radical cation [36,37]. Furthermore, the stepwise hydration energies measured for the acetylene trimer ion are also identical to those measured for the benzene cation [37]. Using a similar strategy, the presence of more than one covalent isomer of the $C_4H_4^{\bullet+}$ ion in ionized acetylene clusters has been established with the predominant ion being the cyclobutadiene radical cation [41]. A similar conclusion has been reached based on the infrared predissociation experiments coupled with harmonic frequency

* Corresponding author. Tel.: +1 804 828 3518.

http://dx.doi.org/10.1016/j.ijms.2014.08.023
1387-3806/

calculations which showed that ionization of acetylene clusters results in the formation of a covalently bound $C_4H_4^{\bullet+}$ "core ion" that most likely has the structure of cyclobutadiene [40]. The infrared predissociation spectra suggest the presence of several isomers of the $C_6H_6^{\bullet+}$ ion including a weak absorption attributed to the formation of the benzene cation [40]. Both the infrared spectroscopy and ion mobility experiments suggest that the structures of the $C_4H_4^{\bullet+}$ and $C_6H_6^{\bullet+}$ ions play important roles in the cluster-mediated chemistry in ionized acetylene clusters [40,41].

Ionized aromatics can also undergo a rich ion–molecule chemistry with acetylene molecules leading to the functionalized aromatics found in organic aerosols, combustion products, soot, meteorites, and interstellar medium [4,7,13–15,24,42,43]. In this context, we studied the gas phase reactions of acetylene with the benzene ($C_6H_6^{+\bullet}$), phenylinum ($C_6H_5^+$), pyridine ($C_5H_5N^{+\bullet}$) and pyrimidine ($C_4H_4N_2^{+\bullet}$) cations over a wide temperature range using the mass-selected ion mobility (drift cell) technique [25,26,38]. In these experiments, the reactant cations are mass-selected (using a quadrupole mass filter) and injected into a drift cell containing pure acetylene vapor or an acetylene-helium vapor mixture at well-defined pressures and temperatures. Residence times of the various ions are measured by monitoring the signals corresponding to each ion as a function of time after injection into the cell. Residence time can be varied between 100 and 1500 μs by changing the voltage gradient in the cell. The reactant and product ions exiting the drift cell are analyzed and detected using a second quadrupole mass spectrometer. The time-resolved studies allow the identification of primary and secondary reaction products and the measurement of rate coefficients [25,26,38].

Through our previous studies we discovered novel reactions of the benzene cation with acetylene molecules over a wide temperature range from 120 to 650 K, demonstrating that benzene ions autocatalyze the conversion of associated acetylene molecules into benzene at low temperatures (120 K), and form naphthalene-type covalent products at high temperatures (650 K) [38]. The barrier to the covalent addition of acetylene to the benzene cation can be eliminated by removing a hydrogen atom from the benzene ring [44–46]. Recently, we provided the first direct evidence for the formation of covalently bonded $C_8H_7^+$ (2-phenyl ethenylium ion) and $C_{10}H_9^+$ (protonated naphthalene) ions by the sequential reactions of acetylene with the phenylium ion at room temperature [25]. We also provided experimental evidence for the sequential reactions of acetylene with the pyridine and pyrimidine cations resulting in the growth of a second ring through the formation of stable N—C bonds, thus providing a mechanism for the formation of nitrogen-containing PAHs [26].

In this paper we investigate the reactions of acetylene with the radical cations of benzonitrile (C_7H_5N), phenylacetylene (C_8H_6), and styrene (C_8H_8). These results are compared with the previously published results on the reactions of acetylene with the benzene, phenyl, pyridine, and pyrimidine cations. Synthetic channels with increased numbers of carbon atoms are found in all the observed reactions leading to the formation of covalently-bonded ions. The observed chemistry under a wide range of experimental conditions, including extreme temperatures as high as 650 K, strongly implies a series of ion–molecule reactions that can lead from a simple molecule such as acetylene to polycyclic organics including those incorporating nitrogen.

The organization of the paper is as follows. In the Section 2, we briefly describe the mass-selected ion mobility system and methods used for measuring the rate coefficients of the bimolecular ion–molecule reactions and the product distributions at different temperatures. The computational methods used for the structural calculations are described in Section 2.1. In the Section 3, we first present a brief summary of the acetylene reactions with the benzene and phenyl cations that we previously investigated at different temperatures (Section 3.1) [25,38]. This summary establishes the covalently bonded nature of the reaction products formed at higher temperatures and provides appropriate reference systems for the comparison with the reactions of benzonitrile, phenylacetylene, and styrene cations studied in the present work. The product distributions at different temperatures, kinetics of the reactions at room temperature, and calculated structures of the most likely product ions are presented and discussed in Sections 3.2, 3.3, and 3.4 for the acetylene reactions with benzonitrile, phenylacetylene, and styrene cations, respectively. In Section 3.5, we provide comparisons of the reactions of these three ions with acetylene with the reactions of the pyridine and pyrimidine cations that we studied previously [26]. These comparisons provide the basis for establishing trends in the reactivity of acetylene with ionized aromatics leading to the formation of polycyclic organic ions. The observed trends in reaction kinetics and the structures of the product ions resulting from the sequential reactions of acetylene with the seven studied organic cations namely benzene ($C_6H_6^{+\bullet}$), phenylinum ($C_6H_5^+$), pyridine ($C_5H_5N^{+\bullet}$), pyrimidine ($C_4H_4N_2^{+\bullet}$), benzonitrile ($C_7H_5N^{+\bullet}$), phenyl acetylene ($C_8H_6^{+\bullet}$), and styrene ($C_6H_8^{+\bullet}$) are examined and discussed in Section 3.6. Finally, in Section 4, we provide an overall summary of the results and highlight the main conclusions of this work.

2. Experimental section

The experiments were performed using the VCU mass-selected ion mobility tandem mass spectrometer (See Fig. 1). The details of the instrument can be found in several publications [25,26,38,47] and only a brief description of the experimental procedure is given here. The molecular ions (styrene $C_8H_8^{\bullet+}$ (m/z 104), phenylacetylene $C_8H_6^{\bullet+}$ (m/z 102), or benzonitrile $C_7H_5N^{\bullet+}$ (m/z 103) were generated by 50 eV EI ionization following the supersonic beam expansion of the corresponding vapor mixture consisting of 0.1–0.2% of the organic vapor (benzonitrile,

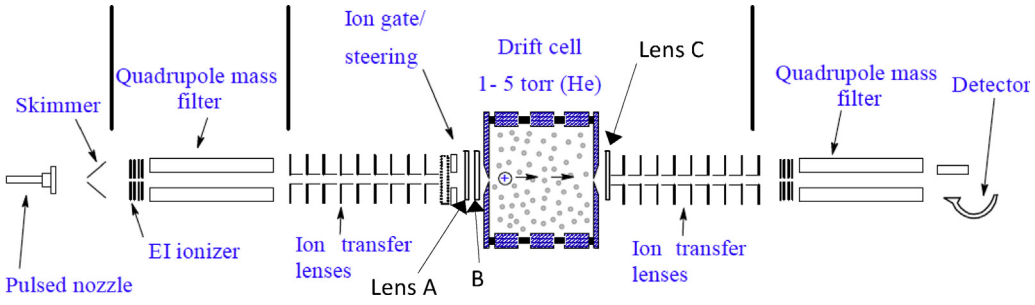

Fig. 1. Schematic diagram of the mass-selected ion mobility tandem mass spectrometer at VCU.

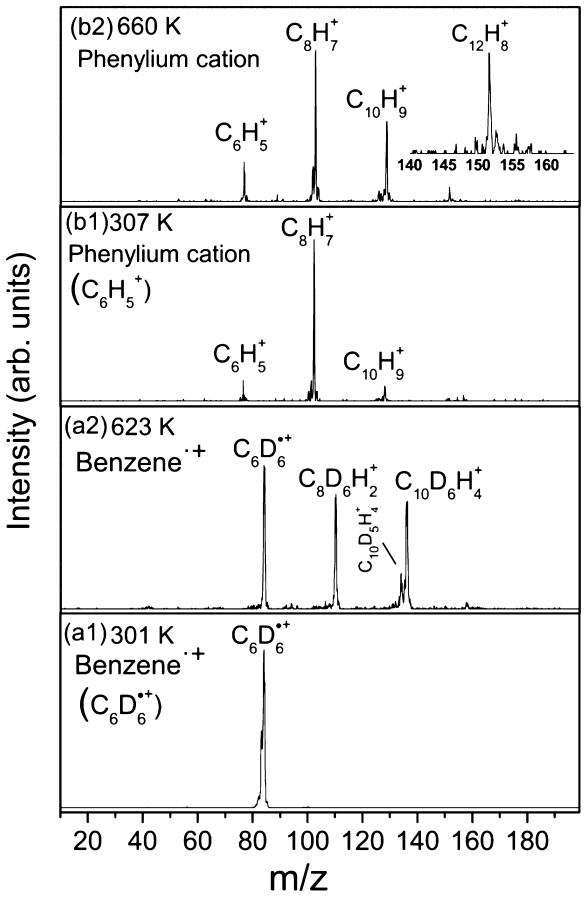

Fig. 2. Temperature dependence of the acetylene reactions with the benzene radical cation ($C_6D_6^{+\bullet}$) at 301 K (a1) and 623 K (a2), and with the phenyl cation ($C_6H_5^+$) at 307 K (b1) and 660 K (b2). In (b1) and (b2) the $C_6H_5^+$ ions were injected into the drift cell containing purified acetylene with pressure of 0.54 Torr at different temperatures. In (a1) and (a2) the $C_6D_6^{+\bullet}$ ions (m/z 84) were injected into the drift cell containing purified acetylene at a cell pressures of 0.35 Torr at the temperatures indicated.

phenylacetylene, or styrene) in 4–5 bar of ultra-pure helium through a 200 μm diameter pulsed nozzle (General Valve, Series 9) in pulses of 150–300 μs duration at repetition rates of 50–100 Hz into a source chamber (10^{-8} mbar). The ions of interest were mass-selected by a quadrupole mass filter and the beam was chopped into small pulses (5–15 μs pulses) and injected into the drift cell (5 cm long) containing a purified acetylene-helium mixture or only purified acetylene gas at known pressures and temperatures. Flow controllers (MKS#1479 A) were used to maintain a constant pressure inside the drift cell within ±1 mTorr. The temperature of the drift cell can be controlled to better than ±1 K using four temperature controllers.

The injection energies used in the experiments (10–14 eV, laboratory frame) are slightly above the minimum energies required to introduce the ions into the cell against the He or C_2H_2/He outflow from the entrance orifice. Most of the ion thermalization occurs outside the cell entrance by collisions with He atoms or C_2H_2 molecules escaping from the cell entrance orifice. Arrival time distributions (ATDs) of the various ions are measured by monitoring the signal corresponding to each ion as a function of time after injection into the cell. Residence time can be varied by changing the voltage gradient in the cell. Pseudo first-order rate constants k_1 are calculated using the following relation, where I is the integrated intensity of the reactant ATD peak and ΣI is the sum of the intensities of the ATDs of reactant and all product ions including the secondary products, and t is the mean drift time taken as the center of the ATD of the reactant ion. k_1 is obtained from the slope of lnI/ΣI versus t, where the reaction time is varied by varying the drift cell voltage. The second-order rate constant k_2 is obtained from $k_2 = k_1/[N]$, where N is the number density (molecules cm^{-3}) of the neutral reactant (C_2H_2) calculated from the measured partial pressure of the reactant inside the drift cell at a given temperature.

All the rate coefficients were replicated several times and the estimated errors are calculated based on the uncertainties in the measurements of the neutral reactant pressure and temperature in addition to fluctuations in ion signal and background noise.

2.1. Computational section

Density functional theoretical (DFT) calculations at the B3LYP exchange-correlation functional level of theory were used to determine the structures and relative energies of the first and second covalent adducts of acetylene with the benzonitrile, phenylacetylene or styrene radical cation using the Gaussian 03 program [48]. This level of theory has been proven to yield sufficiently accurate and reliable results on similar systems [26,47,49,50]. The geometry optimizations and energy calculations were done using the fairly large 6-311++G** basis set which includes *d*-type and *p*-type polarization functions on non-hydrogen and hydrogen atoms, respectively and also have all electrons included [51]. The starting geometries of the first addition of acetylene to the benzonitrile, phenylacetylene, and styrene radical cations were obtained by considering all the possible addition sites on the radical ion where the acetylene molecule could covalently bound. The lowest energy isomers obtained for the first covalent adducts were then used as the starting points for the second addition of acetylene to form the second covalent adducts. To ensure that ground state structures were obtained, vibrational frequency analysis was performed at 298 K to verify the absence of any imaginary frequencies, which indicate the presence of transition states. All the energies obtained from the frequency calculation were corrected for zero point vibrational energy (ZPVE).

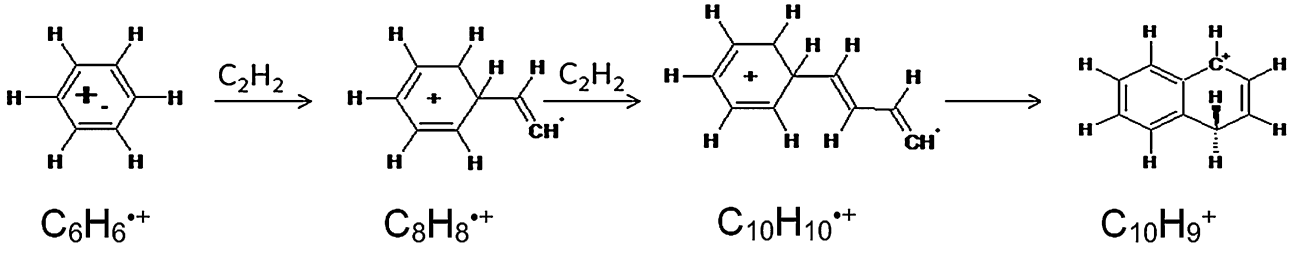

Fig. 3. Reaction mechanism for the formation of naphthalene-type ion ($C_{10}H_9^+$) by the sequential reactions of acetylene with the benzene radical cation at high temperatures [38].

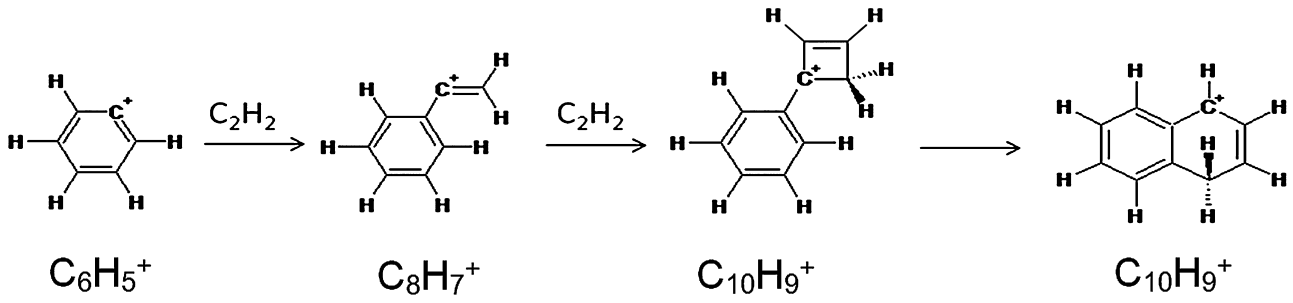

Fig. 4. Reaction mechanism for the formation of protonated naphtalene ($C_{10}H_9^+$) by the sequential reactions of acetylene with the phenyl cation ($C_6H_5^+$) and rearrangements of the stepwise product ions [25].

3. Results and discussion

3.1. Sequential reactions of acetylene with the benzene and phenylium cations

Under ordinary conditions at 300 K, the benzene cation does not react with acetylene as shown in Fig. 2(a1) [38], in agreement with previous work [52]. The temperature dependence of the product distributions of the acetylene reactions with the benzene and the phenyl cations are shown in Fig. 2. Although no products are observed from the acetylene reaction with the benzene cation at room temperature as shown in Fig. 2(a1), Reactions (1) and (2) apparently leading to covalent adducts are observed at higher temperatures as shown in Fig. 2(a2) [38].

$$C_6D_6^{+\bullet} + HCCH \rightarrow C_8D_6H_2^{+\bullet} \quad (1)$$

$$C_8D_6H_2^{+\bullet} + HCCH \rightarrow C_{10}D_6H_4^{+\bullet} \quad (2a)$$

$$\rightarrow C_{10}\ D_5H_4^{+} + D \quad (2b1)$$

$$\text{or} \rightarrow C_{10}\ D_6H_2^{+} + H_2 \quad (2b2)$$

The presence of an energy barrier is confirmed by measuring the overall rate coefficient for the disappearance of $C_6D_6^{+\bullet}$ (m/z 84), and the generation of the first adduct $C_8D_6H_2^{+\bullet}$ (m/z 110), the second adduct $C_{10}D_6H_4^{+\bullet}$ (m/z 136) and $C_{10}D_5H_4^{+\bullet}$ (m/z 134) at higher temperatures [38]. The second-order rate coefficient measured within the temperature range of 470 K to 670 K is $(3 \pm 0.7) \times 10^{-13}$ cm^3 s^{-1} indicating a collision efficiency of only 0.0001, and the Arrehenius plot yields a positive activation energy of 3.5 kcal/mol [38].

In contrast to the lack of reactivity of acetylene with the benzene cation at room temperature, the phenyl cation shows high reactivity with acetylene at both room and higher temperatures. The sequential addition of acetylene onto the phenylium ion is evident from the appearance of the first and second adducts ($C_8H_7^+$ and $C_{10}H_9^+$, respectively) at room temperature as shown in Fig. 2(b1). At higher pressure of acetylene (0.79 Torr) at 300 K the third adduct $C_{12}H_{11}^+$ starts to appear while at the same conditions no addition is observed on the benzene cation [25]. The product ions $C_8H_7^+$, $C_{10}H_9^+$, and $C_{12}H_{11}^+$ formed at room temperature are covalent adducts since the formation of ion–molecule association complexes would require much lower temperatures as a result of the weak charge-induced dipole interaction. For example, the association complexes of acetylene with the benzene cation [$C_6D_6^{+\bullet}(C_2H_2)_n$, n = 1–4] were observed in 0.50 Torr acetylene only at temperatures below 160 K due to the weak binding energies of 3–4 kcal/mol [49].

For the acetylene reaction with the phenyl cation, a significant increase in the intensity of the second adduct ($C_{10}H_9^+$) is observed when the temperature of the drift cell increases from 307 to 660 K as shown in Fig. 2(b1 and b2) [25]. This observation confirms the covalent nature of the phenylium ion-acetylene adducts since ion–molecule clusters involving weak ion-induced dipole interactions would not survive at such higher temperatures. Interestingly, above 600 K, the intensity of the third adduct $C_{12}H_{11}^+$ decreases and a new peak corresponding to the ion $C_{12}H_8^+$ appears as shown in Fig 2(b2). This suggests an endothermic rearrangement of the adduct $C_{12}H_{11}^+$ by the elimination of an H atom and H_2 molecule to generate a more stable $C_{12}H_8^+$ ion which could correspond to the radical cation of 1-naphthylacetylene or the polycyclic acenaphthalene [25].

The structures of the covalent adducts formed by the high temperature reactions of acetylene with the benzene cation have

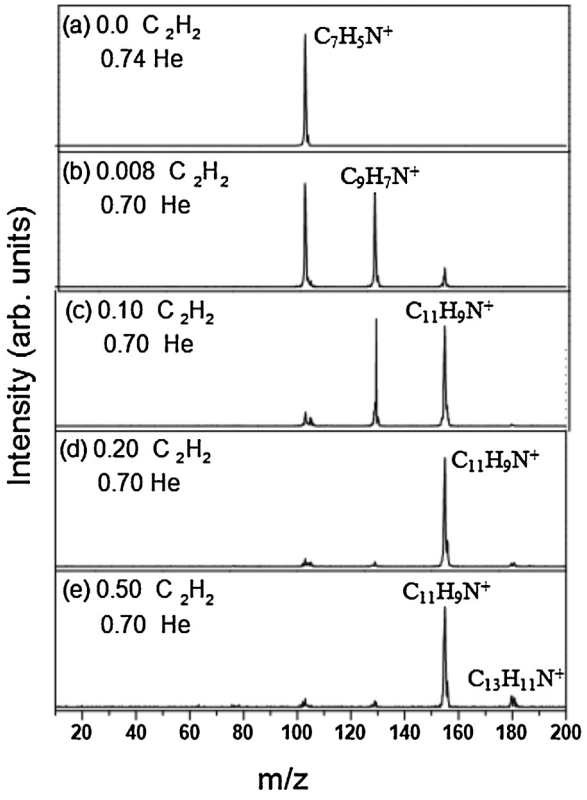

Fig. 5. Mass spectra obtained following the injection of the benzonitrilecation ($C_7NH_5^{+\bullet}$) into the drift cell at 299 K. Drift cell pressures (in Torr) are shown.

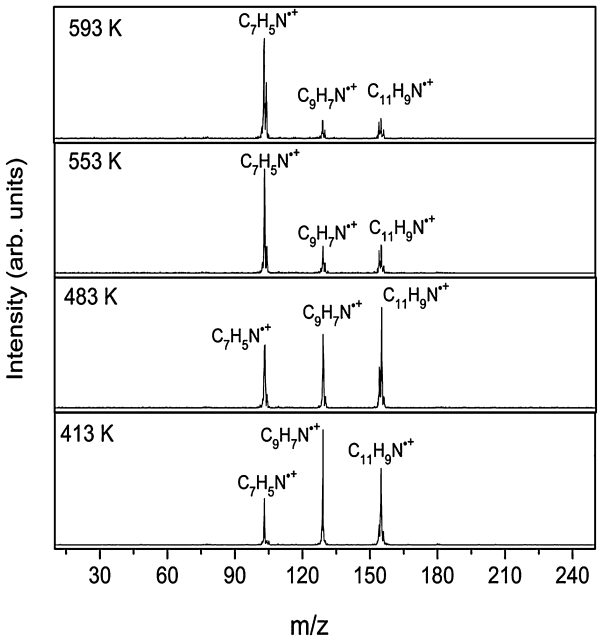

Fig. 6. Mass spectra showing the product distributions following the injection of the benzonitrile cation ($C_7NH_5^{\bullet+}$) into the drift cell containing 0.12 Torr C_2H_2 and 0.64 Torr helium at different temperatures as indicated.

been studied by DFT calculations [38]. The structures of the first adduct $C_8H_8^{+\bullet}$, the second adduct $C_{10}H_{10}^{+\bullet}$ and $C_{10}H_9^+$ product obtained at the B3LYP/6-31G* level are shown in Fig. 3 [38]. According to the DFT calculations, the formation of the $C_{10}H_{10}^{+\bullet}$ ion by the addition of acetylene to the $C_8H_8^{+\bullet}$ ion is quite exothermic and does not involve a barrier [38]. Furthermore, the abstraction of H from the $C_{10}H_{10}^{+\bullet}$ ion by another H to form the naphthalene structure ($C_{10}H_9^+$) occurs in an exothermic and barrierless process [46]. Since the formation of the second adduct $C_{10}H_{10}^{+\bullet}$ is barrierless, the experimentally observed barrier (3.5 kcal/mol) can be attributed to the formation of the first adduct $C_8H_8^{+\bullet}$ which is the most likely rate-limiting step for formation of the naphthalene-type ion $C_{10}H_9^+$ (protonated naphthalene) [38].

For the acetylene reaction with the phenyl cation, DFT calculations at the UPBEPBE/6-31 ++G** level identify the first adduct $C_8H_7^+$ in the acetylene reactions with the phenyl cation as 2-ethenylium ion, the most stable $C_8H_7^+$ isomer that maintains the phenylium ion structure, as shown in Fig. 4 [25]. The addition of the second acetylene on the phenyl cation is predicted to be exothermic (by 56.7 kcal/mol) and to involve a very small barrier of 0.6 kcal/mol leading to the formation of a four-membered ring adduct $C_{10}H_9^+$ as shown in Fig. 4 [46]. This structure is also found to be the most stable $C_{10}H_9^+$ isomer that maintains the phenylium ion structure at the UPBEPBE/6-31 ++G** level [25].

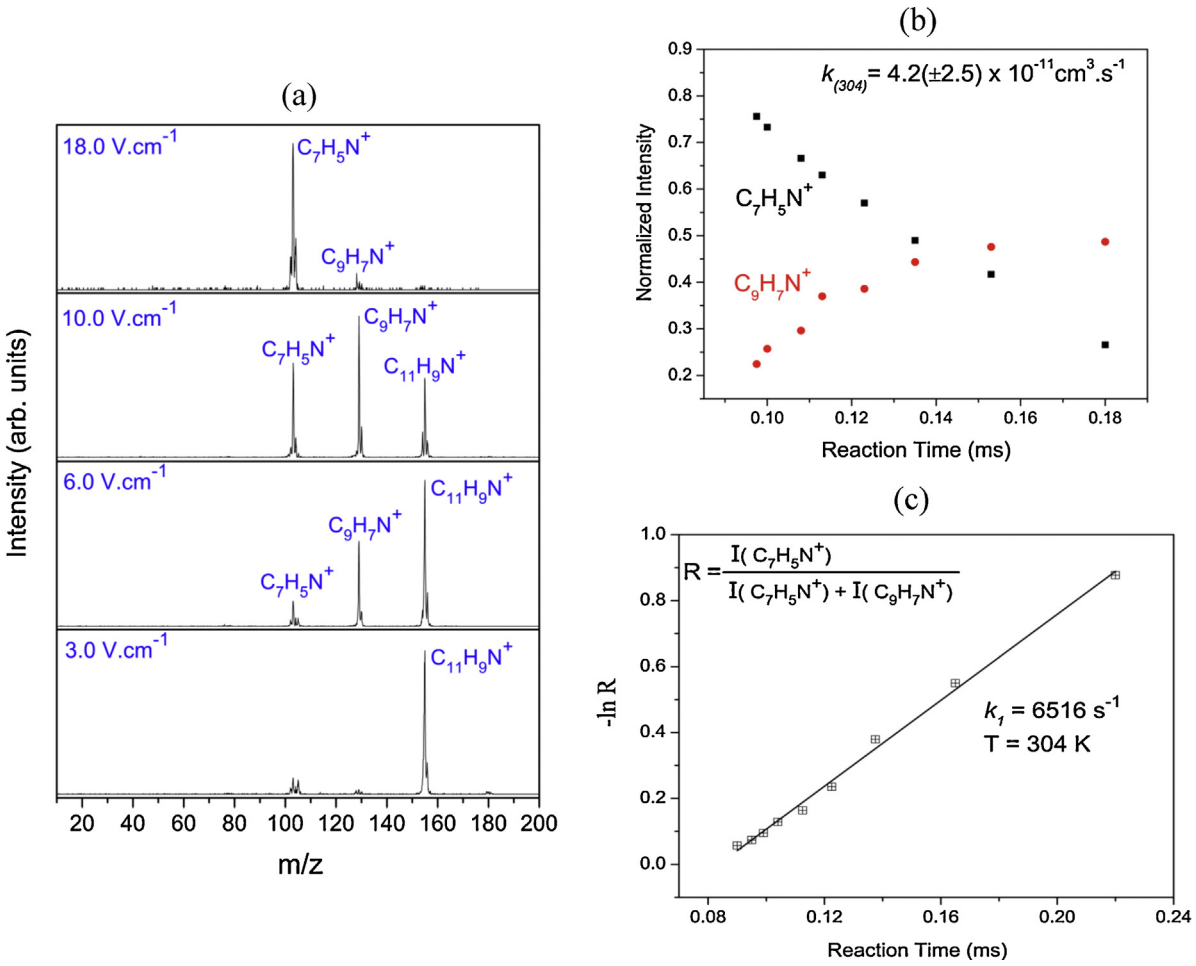

Fig. 7. (a) Effect of drift field on the observation of the reaction products following the injection of benzonitrile radical cation ($C_7NH_5^{\bullet+}$) into the drift cell containing 0.10 Torr acetylene (C_2H_2) and 0.50 Torr He at 300 K. (b) Integrated arrival time distributions of the reactant and product ions as a function of reaction time following the injection of benzonitrilecation (C7NH5$^{\bullet+}$) into the drift cell containing 0.005 Torr acetylene in 0.515 Torr helium at 304 K. (c) Pseudo first order rate constant calculated from the slope of the semi-log plot of the normalized ion intensity of the reactant ion ($C_7NH_5^{\bullet+}$) under the same conditions of Fig. 7-b.

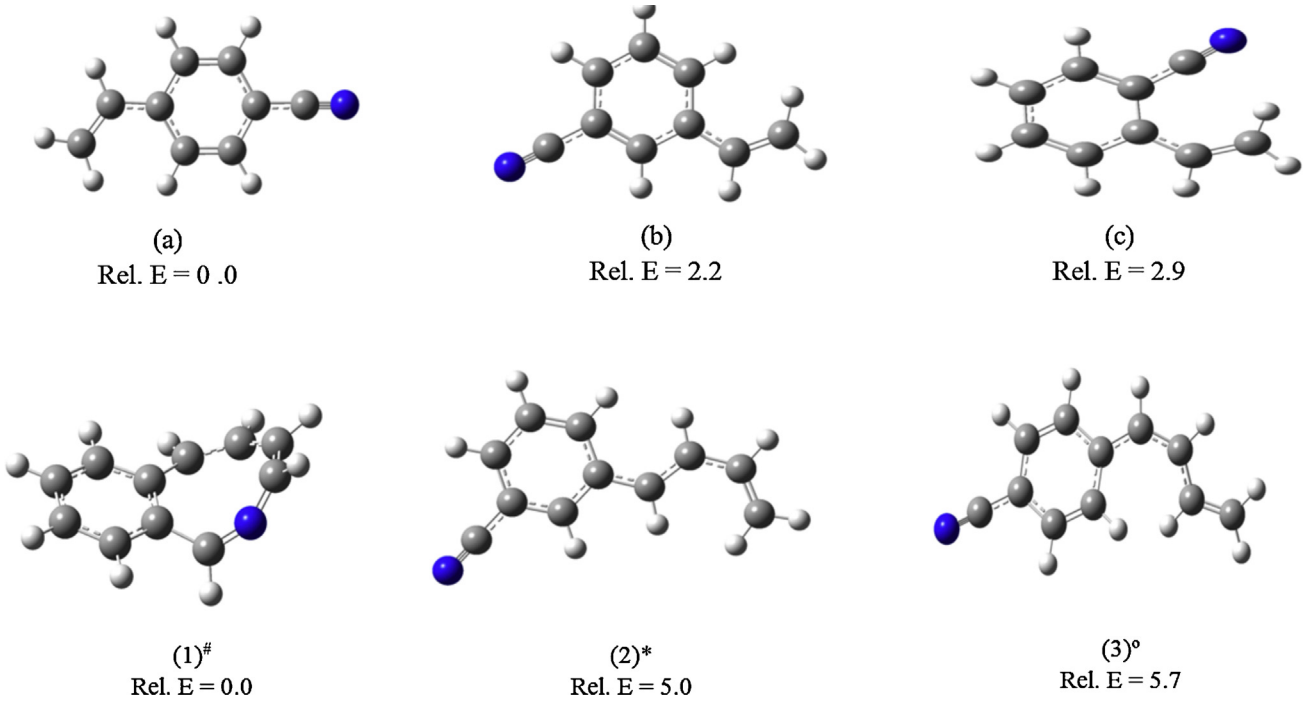

Fig. 8. Calculated covalent structures of the $C_9NH_7^{\bullet+}$ and $C_{11}NH_9^{\bullet+}$cations with their relative energies (kcal/mol) obtained at the B3LYP/6–311 + +G** level of theory. #, * and ◦ indicate structures resulting from the acetylene addition to isomers (c), (b) and (a), respectively of the $C_9NH_7^{\bullet+}$ ion.

3.2. Reactions of acetylene with the benzonitrile radical cation

Fig. 5 displays the mass spectra obtained following the injection of the benzonitrile radical cation ($C_7NH_5^{\bullet+}$) into the drift cell containing 0.70 Torr helium and variable amounts of acetylene at room temperature. As shown in Fig. 5(a), in the presence of pure helium, only the molecular benzonitrile ion is observed with no fragmentation confirming the absence of excess ionization and injection energies which could lead to the fragmentation of the ion. EI ionization of benzonitrile under the high pressure conditions of the supersonic beam expansion of the benzonitrile/helium mixture leads to the deposition of a small amount of energy on

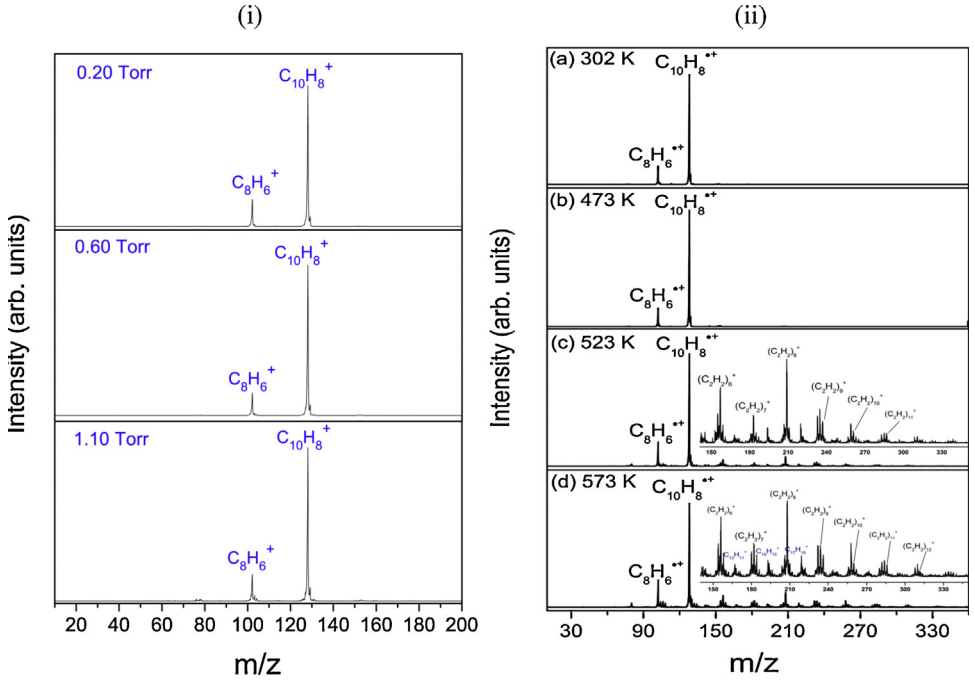

Fig. 9. (a) Mass spectra obtained following the injection of the mass-selected phenylacetylene radical cations ($C_8H_6^{\bullet+}$) into the drift cell containing different acetylene pressures at 302 K. (b) Temperature dependence of the acetylene reactions with the phenylacetylene radical cation following the injection of the mass-selected $C_8H_6^{\bullet+}$ ions into the drift cell containing 0.62 Torr purified C_2H_2.

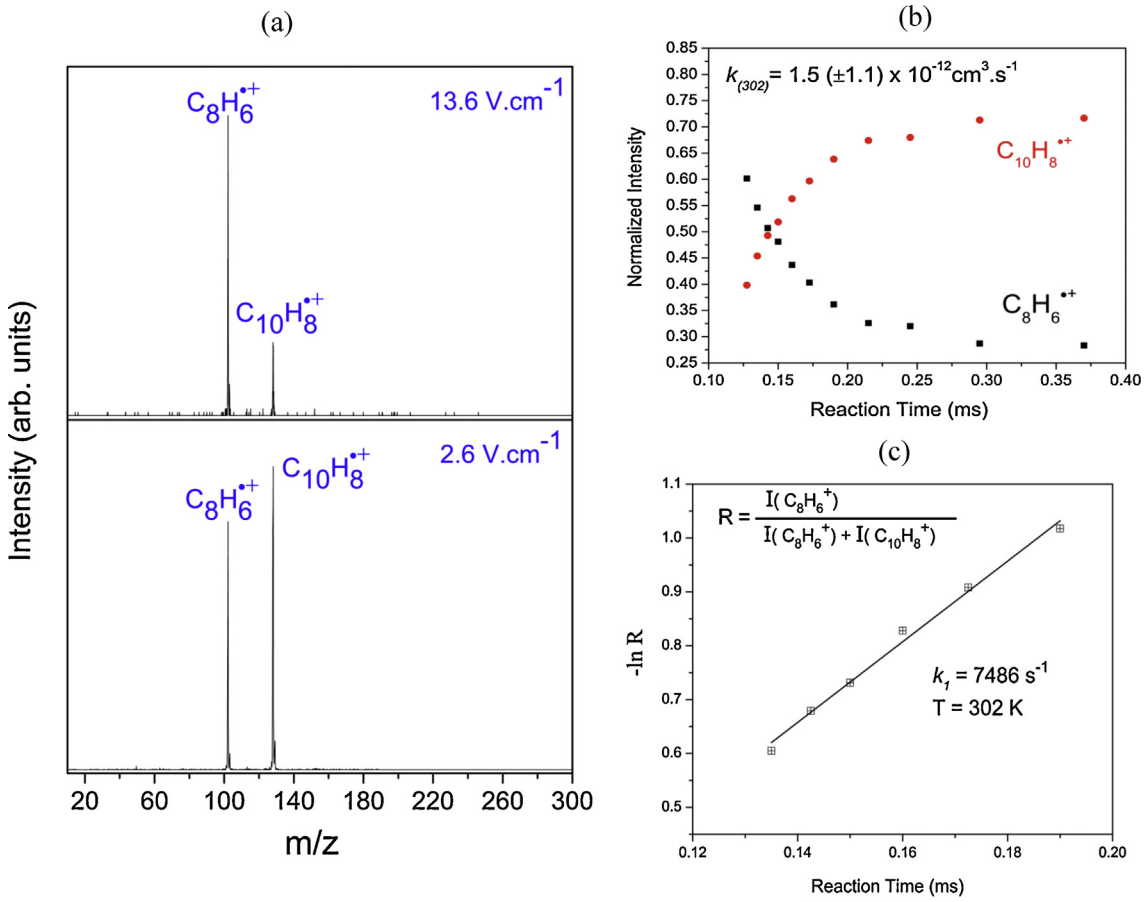

Fig. 10. (a) Effect of drift field on the observation of the reaction products following the injection of phenylacetylene radical cation ($C_8H_6^{\bullet+}$) into the drift cell containing 0.06 Torr acetylene (C_2H_2) and 0.91 Torr He at 302 K. (b) Integrated arrival time distributions of the reactant and product ions as a function of reaction time following the injection of thr $C_8H_6^{\bullet+}$ into the drift cell containing 0.06 Torr acetylene in 0.91 Torr helium at 302 K. (c) Pseudo first order rate constant calculated from the slope of the semi-log plot of the normalized ion intensity of the reactant ion $C_8H_6^{\bullet+}$ under the same conditions of Fig. 10(b).

the ions as evident by the absence of any fragments upon the injection of the ions into the drift cell. At a very low pressure of C_2H_2 (0.008 Torr), the first adduct $C_9NH_7^{\bullet+}$ (*m*/*z* 129) is readily formed as shown in Fig. 5(b). By increasing the acetylene pressure to 0.1 Torr, the benzonitrile radical cation ($C_7NH_5^{\bullet+}$) reacted almost completely with acetylene to produce the first and second adducts ($C_9NH_7^{\bullet+}$ (*m*/*z* 129) and $C_{11}NH_9^{\bullet+}$ (*m*/*z* 155), respectively) as the two major products in addition to a small amount of the third adduct $C_{13}NH_{11}^{\bullet+}$ (*m*/*z* 181) as shown in Fig. 5(c). It should be noted that the product distribution of the adducts formed depends strongly on the pressure of acetylene in the drift cell. At low pressures (0.01–0.10 Torr), the first two adducts $C_9NH_7^{\bullet+}$ and $C_{11}NH_9^{\bullet+}$ are observed as shown in Fig. 5(b and c). However, as the pressure of acetylene increases (0.20 Torr, Fig. 5(d)), the second adduct $C_{11}NH_9^{\bullet+}$ becomes the most abundant ion and even at a higher pressure such as 0.50 Torr acetylene, the third adduct $C_{13}NH_{11}^{\bullet+}$ is formed with a small intensity as shown in Fig. 5(e). This suggests that the adduct ion $C_{11}NH_9^{\bullet+}$ formed by the sequential addition of two acetylene molecules onto the benzonitrile radical cation may represent a terminated product with low reactivity towards the addition of further acetylene molecules.

Fig. 6 displays the mass spectra obtained following the injection of the benzonitrile cation ($C_7NH_5^{\bullet+}$) into the drift cell containing 0.64 Torr helium and 0.12 Torr C_2H_2 at different temperatures. It is clear that the two adducts $C_9NH_7^{\bullet+}$ (*m*/*z* 129) and $C_{11}NH_9^{\bullet+}$ (*m*/*z* 155) can be observed at temperatures as high as 593 K consistent with the covalent nature of these ions. However, the relative ion intensities of the two adduct ions decrease and that of the hydrogen-abstracted benzonitrile ion ($C_7NH_6^+$) increases at temperatures above 550 K. This could reflect the presence of a mixture of isomers of the $C_9NH_7^{\bullet+}$ and $C_{11}NH_9^{\bullet+}$ ions where some structures may have low thermal stability and may dissociate by the loss of C_2H and C_4H_3 radicals, respectively to produce the $C_7NH_6^+$ ions at temperatures above 550 K.

The time-dependent product distribution at 300 K is determined by changing the voltage gradient in the drift cell as shown in Fig. 7(a). By decreasing the voltage gradient in the drift cell (3.0 V/cm), the residence time of the ions inside the drift cell increases which results in increasing the product yield into the two adduct ions $C_9NH_7^{\bullet+}$ and $C_{11}NH_9^{\bullet+}$ as shown in Fig. 7(a). This is consistent with irreversible reactions leading the formation of covalent ions as suggested by the concentration and temperature dependences of the product ions. To measure the second order rate coefficient due mostly to the first adduct, the reactant ion ($C_7NH_5^{\bullet+}$) is injected into the drift cell containing a very small pressure of acetylene (0.005 Torr) in the presence of 0.515 Torr helium as a third body buffer gas as shown in Fig. 7(b). Under these conditions, there is almost no contribution to the total ion intensity observed during the residence time from the second adduct. Pseudo first order rate coefficient calculated from the slope of the semi-log plot of the normalized intensity of the $C_7NH_5^{\bullet+}$ ion is shown in Fig. 7(c). The rate coefficient shows no pressure dependence of the carrier gas within the measured range from 0.2–1.0 Torr helium indicating

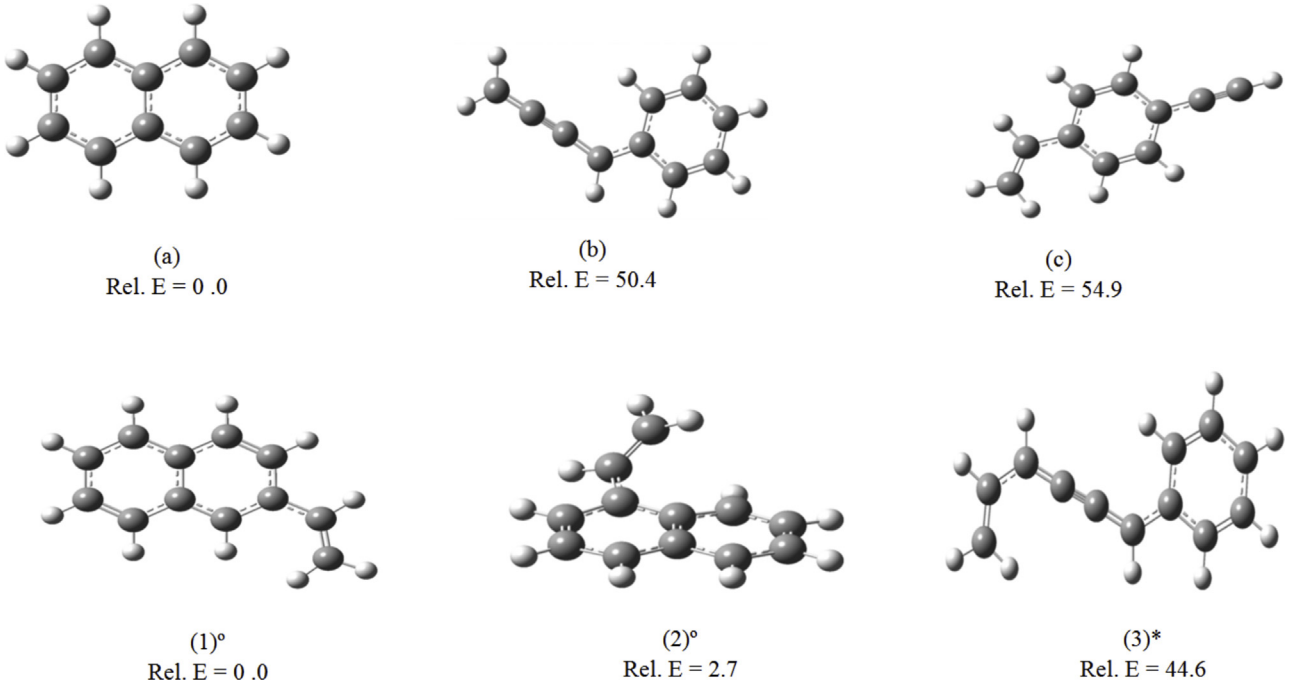

Fig. 11. Calculated covalent structures of the $C_{10}H_8^{\bullet+}$ and $C_{12}H_{10}^{\bullet+}$ ions formed by the acetylene reactions with the phenylacetylene radical cation ($C_8H_6^{\bullet+}$) and their relative energies (kcal/mol) obtained at the B3LYP/6-311 ++G** level of theory. ° and * indicate structures resulting from the acetylene addition onto isomers (a) and (b), respectively of the $C_{10}H_8^{\bullet+}$ ion.

that the reaction is second-order. The measured rate coefficient of 4.2 ($\pm$2.5) $\times$ 10^{-11} cm^3 s^{-1}) indicates a reaction efficiency (defined here as the ratio of the measured rate coefficient to the Langevin capture rate coefficient taken as 1.5 $\times$ 10^{-9} cm^3 s^{-1}) of nearly 2.8% at 304 K. The higher reactivity of the benzonitrile cation towards acetylene is in contrast to the very low reaction efficiency (10^{-4}–10^{-5}) observed for the addition of acetylene on the benzene cation [38]. This confirms that the barrier to the cation ring growth can be reduced or overcome by introducing appropriate substituent groups in the cation ring [44–46]. Thus, nitrogen-containing complex organics can be produced by the sequential reactions of acetylene with the benzonitrile cation at room temperature and relatively high pressure conditions (0.1 Torr).

The structures of the three lowest energy covalent ions formed by the reaction of acetylene with the benzonitrile cation obtained at the B3LYP/6-311 ++G** level of theory are shown in Fig. 8 as isomers (a), (b) and (c). Additional higher energy isomers are shown in Fig. S1 (Supporting information). The three lowest energy isomers (a), (b) and (c) have similar energies (within 3 kcal/mol) and represent the addition of acetylene on the para, meta and ortho positions, respectively of the benzonitrile cation. Isomers involving proton transfer from the ortho and para positions of the ring hydrogens to the nitrogen atom of the nitrile group with the addition of acetylene to the ring are found to be at 10–26 kcal/mol higher energy than isomer (a) (see Fig. S1). Other isomers involving the addition of acetylene directly on the nitrogen atom of the benzonitrile cation are found to be 27–47 kcal/mol higher in energy than isomer (a) (see Fig. S1, Supporting information).

The structures of the second covalent adduct $C_{11}H_9N^{\bullet+}$ were obtained by locating the lowest energy structures resulting from the addition of acetylene to isomers (a), (b) and (c) shown in Fig. 8. The resulting three lowest energy isomers of the $C_{11}H_9N^{\bullet+}$ ion are shown in Fig. 8 as isomers (1), (2), and (3), and all the 17 low energy isomers found for the $C_{11}H_9N^{\bullet+}$ ion are given in Fig. S2 (Supporting information). Interestingly, the lowest energy isomer of the $C_{11}H_9N^{\bullet+}$ ion (1), formed by the addition of acetylene to the (c) isomer of the $C_9NH_7^{\bullet+}$ ion, contains an expanded fused ring structure as shown in Fig. 8 (structure (1)#). This structure could account for the termination of the acetylene reactions with the benzonitrile cation after the second addition. The other two isomers (2)* and (3)° of the $C_{11}H_9N^{\bullet+}$ ion have similar energies and represent the addition of acetylene to isomers (b) and (c), respectively of the $C_9H_7N^{\bullet+}$ ion as shown in Fig. 8.

3.3. Reactions of acetylene with the phenylacetylene radical cation

The phenylacetylene radical is believed to form naphthalene upon reactions with acetylene [53]. Several studies suggest the possibility of producing a phenylacetylene ion through a loss of an acetylene molecule from the naphthalene radical cation [54–56]. The $C_8H_6^{\bullet+}$ produced by the loss of an acetylene molecule from the naphthalene radical cation could also have the structure of benzocyclobutadiene which is only 4 kcal/mol higher in energy than the phenylacetylene isomer [56].

Injection of the phenylacetylene radical cations ($C_8H_6^{\bullet+}$) into the drift cell containing acetylene at room temperature resulted in the formation of the $C_{10}H_8^{\bullet+}$ ion (m/z 128) as shown in Fig. 9(a), which could be have the naphthalene ion structure [53]. No further acetylene additions were observed when the acetylene pressure in the drift cell was increased from 0.20 to 1.1 Torr as shown in Fig. 9 (a). This is consistent with the formation of stable naphthalene radical cation which may react with acetylene at higher temperatures similar to the reaction of the benzene cation with acetylene [38]. In fact, the acetylene reactions with phenylacetylene cation show strong temperature dependence as shown in Fig. 9(b). When the temperature of the drift cell was increased from 302 to 573 K, higher acetylene additions on the first adduct $C_{10}H_{10}^{\bullet+}$(presumably naphthalene cation) $C_{10}H_{10}^{\bullet+}(C_2H_2)_n$ with n up to 10 were observed as shown in Fig. 9(b). Interestingly, another series containing odd number of carbon atoms ($C_{11}H_9^+$, $C_{13}H_{11}^+$, $C_{15}H_{13}^+$, etc.) was also

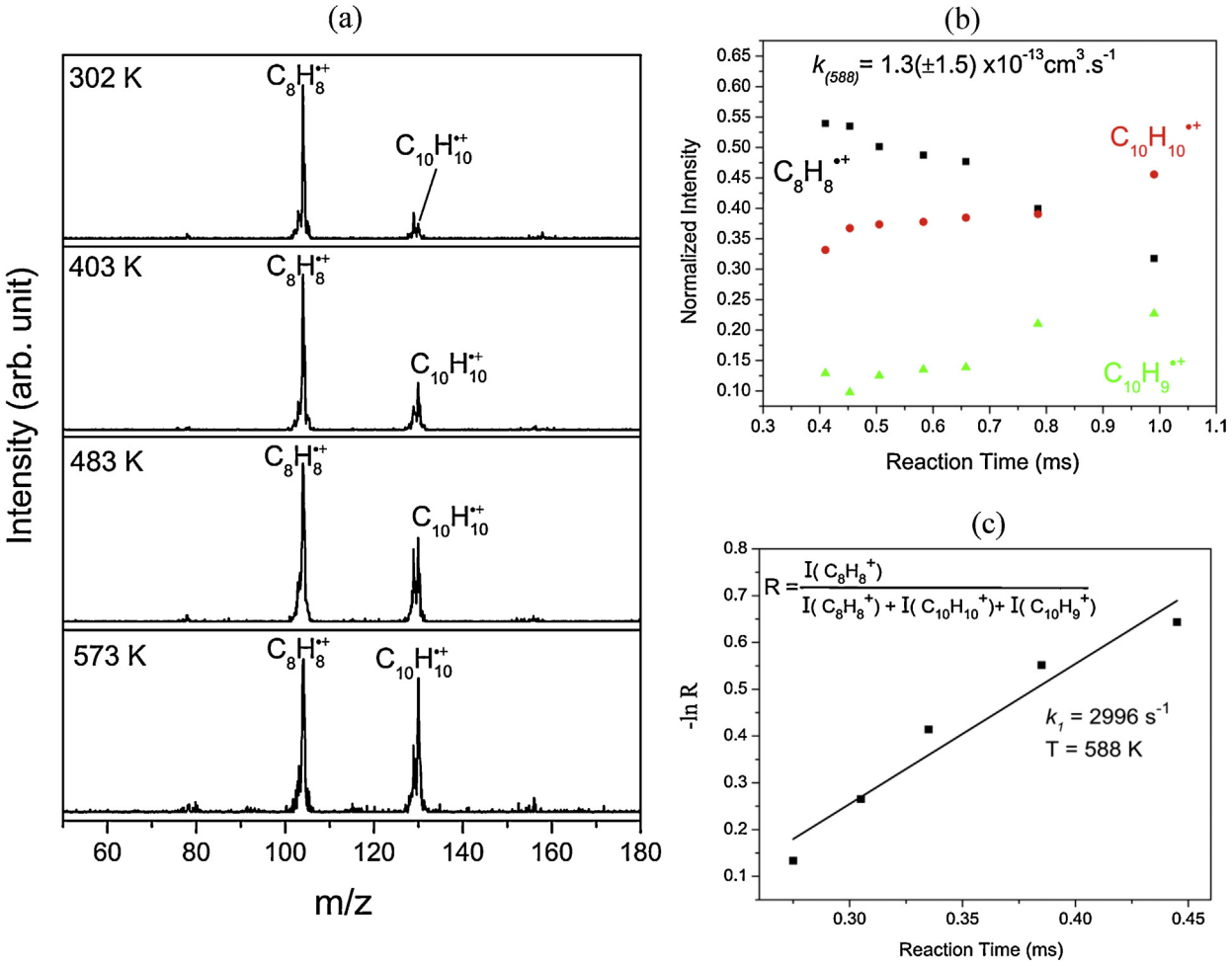

Fig. 12. (a) Temperature dependence of the acetylene reactions with the styrene radical cationfollowing the injection of the mass-selected $C_8H_8^{\bullet+}$ ions into the drift cell containing 0.69 Torr purified C_2H_2. (b) Integrated arrival time distributions of the reactant and product ions as a function of reaction time following the injection of thr $C_8H_8^{\bullet+}$ into the drift cell containing 0.85 Torr acetylene at 588 K. (c) Pseudo first order rate constant calculated from the slope of the semi-log plot of the normalized ion intensity of the reactant ion $C_8H_8^{\bullet+}$ under the same conditions of Fig. 12(b).

observed at higher temperatures as shown in Fig. 9(b). The formation of the polymer sequence containing odd number of carbon atoms suggests the elimination of C7 neutral species from the growing adduct series $C_{10}H_{10}^{\bullet+}(C_2H_2)_n$ with $n \geq 4$. This assumption could be tested by investigating the reactions of the naphthalene radical cation with acetylene at higher temperatures. These experiments are currently underway in order to determine the nature of the acetylene polymer ions formed from the acetylene reactions with the phenylacetylene cation at higher temperatures.

The time-dependent product distribution at 302 K determined by changing the voltage gradient in the drift cell as shown in Fig. 10 (a). No other products except the first adduct $C_{10}H_8^{\bullet+}$ was observed at room temperature even at the longest reaction time and highest pressure of acetylene used in the experiments (1.1 Torr). The time profiles of the reactant ($C_8H_6^{\bullet+}$) and product ($C_{10}H_8^{\bullet+}$) ions following the injection of the reactant ions into the drift cell containing a small pressure of acetylene (0.06 Torr) in 0.91 Torr are shown in Fig. 10(b). Pseudo first order rate coefficient calculated from the slope of the semi- log plot of the normalized intensity of the $C_8H_6^{\bullet+}$ ion is shown in Fig. 10(c). The measured rate coefficient of 1.5 ($\pm$1.1) $\times$ 10^{-12} cm^3 s^{-1} at 302 K shows no dependence on the pressure of the helium carrier gas within the range of 0.3–1.0 Torr indicating that the reaction is second-order. The higher reactivity of the benzonitrile cation as compared to the phenylacetylene cation towards acetylene could be due to the electron withdrawing ability of the nitrile group which could make the ring more reactive for the addition of acetylene.

The structures of the three lowest energy covalent ions formed by the reaction of acetylene with the phenylacetylene cation obtained at the B3LYP/6-311 ++G** level of theory are shown in Fig. 11 as isomers (a), (b), and (c). Additional higher energy isomers are shown in Fig. S3 (Supporting information). As expected, the lowest energy isomer of the $C_{10}H_8^{\bullet+}$ ion is the naphthalene cation with a significantly lower energy of more than 50 kcal/mol than the energies of the other two acyclic isomers (b) and (c). Another high energy isomer (57.5 kcal/mol above (a)) shows the formation a four-membered ring attached to the phenyl ring as shown in Fig. S3 (Supporting information). The two lowest energy isomers (1 and 2°) of the $C_{12}H_{10}^{\bullet+}$ ion have the structures of substituted naphthalene ion and have significantly lower energies than the acyclic isomer (3)* as shown in Fig. 11. Additional higher energy isomers of the $C_{12}H_{10}^{\bullet+}$ ion are shown in Fig. S4 (Supporting information). Since no second adduct was observed in the acetylene reaction with the phenylacetylene cation at room temperature, it appears that the addition of acetylene on the naphthalene cation could involve energy barriers which may be overcome only at higher temperatures. The acetylene reactions

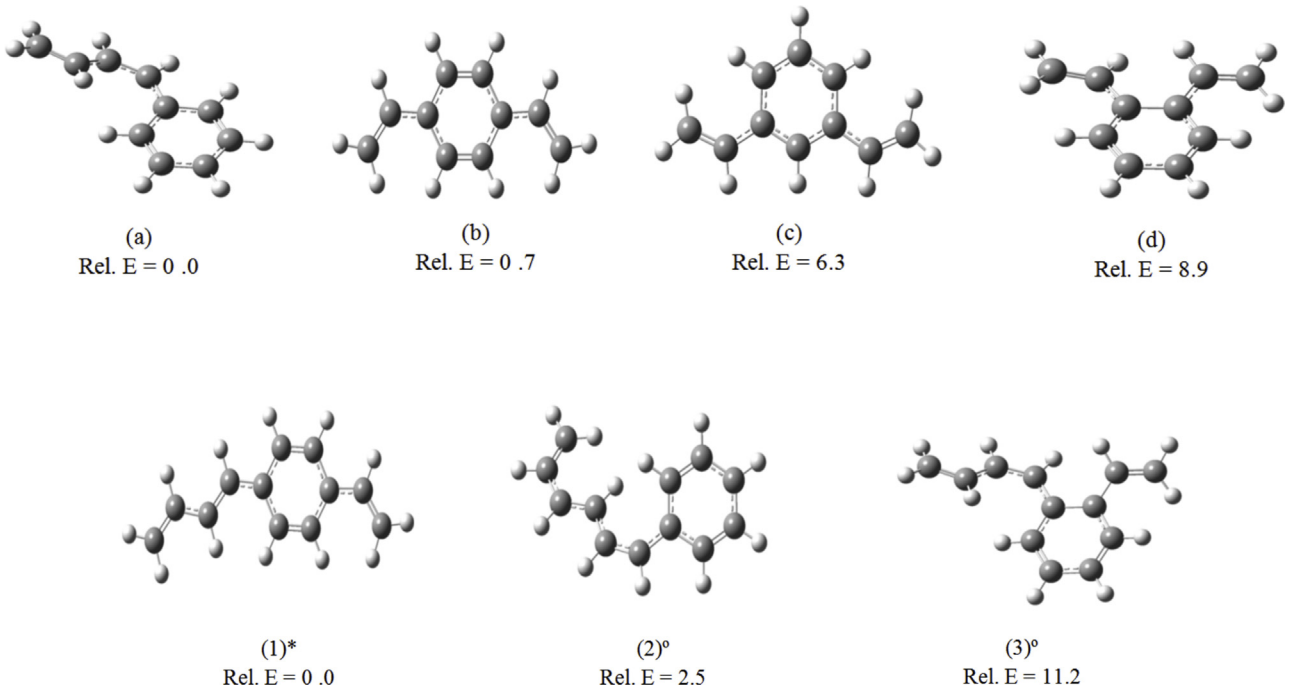

Fig. 13. Calculated covalent structures of the $C_{10}H_{10}^{\bullet+}$ and $C_{12}H_{12}^{\bullet+}$ ions formed by the acetylene reaction with the styrene radical cation ($C_8H_8^{\bullet+}$) and their relative energies (kcal/mol) obtained at the B3LYP/6-311 ++G** level of theory. ◦ and * indicate structures resulting from the acetylene addition onto isomers (a) and (b), respectively of the $C_{10}H_{10}^{\bullet+}$ ion.

with the (actual) naphthalene cation at higher temperatures are currently under investigation in our laboratory.

3.4. Reactions of acetylene with the styrene radical cation

In contrast to the low pressure ICR experiments that resulted in no reactions between styrene radical cation and acetylene [57], we observed that the styrene cation reacts with acetylene at room temperature resulting in the formation of $C_{10}H_9^+$ and $C_{10}H_{10}^{\bullet+}$ cations as shown in Fig. 12(a). A significant increase in the ion intensity of the $C_{10}H_{10}^{\bullet+}$ adduct is observed at higher temperatures as shown in Fig. 12(a) suggesting the presence of an energy barrier for the formation of this ion. It should be noted that no acetylene association products (non-covalent) onto the $C_8H_8^{\bullet+}$, $C_{10}H_9^+$, or the $C_{10}H_{10}^{\bullet+}$ cation were observed at temperatures as low as 130 K as shown in Fig. S5 (Supporting information). The lack of association products indicates weaker interactions between acetylene and these ions as compared to the interaction of acetylene with the benzene cation where the $C_6D_6^{\bullet+}(C_2H_2)$ binding energy was measured as 3.8 kcal mol [49]. The difference in the binding energies of acetylene to the benzene and styrene cations could be due to the smaller ΔIE of 2.2 eV (difference between ionization energies (IEs) of acetylene and benzene) as compared to 2.9 eV for the difference between IEs of acetylene and styrene. The smaller ΔIE allows a partial charge transfer in the $C_6D_6^{\bullet+}(C_2H_2)$ complex which would contribute to increasing the binding energy of the $C_6D_6^{\bullet+}(C_2H_2)$ complex. This indicates that the ions resulting from the room temperature reactions of acetylene with the styrene cation ($C_{10}H_9^+$ and $C_{10}H_{10}^{\bullet+}$) are covalently-bonded adducts. The lack of acetylene association with these ions at low temperatures suggests that the neutral molecules of these ions may have IEs comparable to that of styrene (8.5 eV).

The time profiles of the reactant ($C_8H_8^{\bullet+}$) and product ($C_{10}H_9^+$ and $C_{10}H_{10}^{\bullet+}$) ions following the injection of the styrene cation into the drift cell containing high pressure of acetylene (0.85 Torr) at 588 K are shown in Fig. 12(b). Pseudo first order rate coefficient calculated from the slope of the semi-log plot of the normalized intensity of the $C_8H_8^{\bullet+}$ ion is shown in Fig. 12(c). The

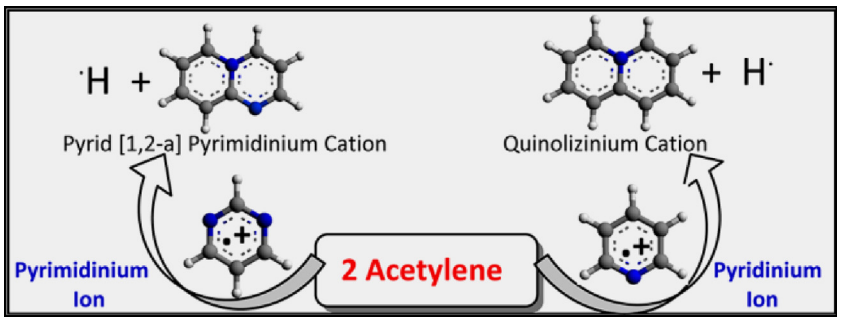

Scheme 1. Formation of nitrogen-containing organic ions by the sequential reactions of acetylene with the pyridine and pyrimidine radical cations.

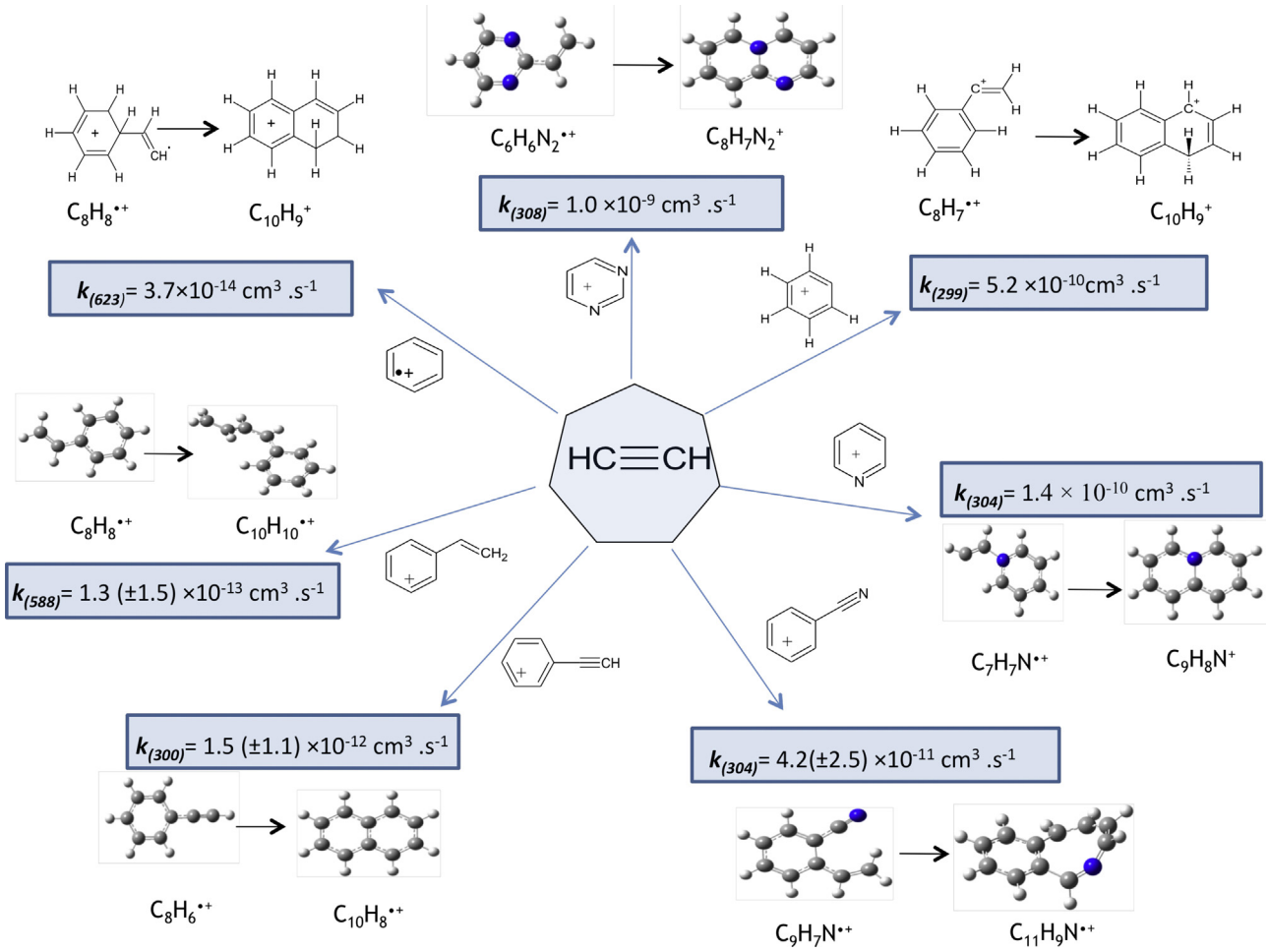

Fig. 14. Overall reaction rates and covalent products formed in the reactions of acetylene with ionized aromatics as shown (for comparison, capture collision rates are usually about 10^{-9} cm^3 s^{-1}).

use of high pressure of acetylene and high reaction temperature (588 K) was necessary due to the slow nature of the reaction. Indeed, the measured rate coefficient of 1.3 (±1.5) × 10^{-13} cm^3 s^{-1}) at 588 K. The low reactivity of the styrene cation towards acetylene is comparable to the reactivity of the benzene cation where a reaction efficiency of 2.5 × 10^{-5} was estimated at 623 K [38].

The structures of the four lowest energy covalent ions formed by the reaction of acetylene with the styrene cation obtained at the B3LYP/6-311 ++G** level of theory are shown in Fig. 13. Two isomers (a) and (b) with similar energies are found as the lowest energy structures of the $C_{10}H_{10}^{\bullet+}$ ion. The first isomer (a) involves the addition of acetylene on the C_2H_3 group of the styrene cation followed by a 1,2 H-shift to form a butylene-substituted benzene cation. The second isomer (b) involves the addition of acetylene in the para position of the styrene ring. Isomers (c) and (d) with higher energies of 6.3 and 8.9 kcal/mol, respectively than isomer (a) show the acetylene addition to occur in the meta and ortho positions, respectively of the styrene ring. The lowest energy isomers of the $C_{12}H_{12}^{\bullet+}$ ion that could be formed by the addition of acetylene to isomers (b), (a), and (a) of the $C_{10}H_{10}^{\bullet+}$ ion are shown as isomers (1)*, (2)°, and (3)°, respectively in Fig. 13. Additional higher energy isomers are shown in Fig. S6 (Supporting Information). Since no second acetylene addition on the styrene cation was observed at room temperature, it appears that the formation of the second adduct $C_{12}H_{12}^{\bullet+}$ involves energy barriers which may be overcome at higher temperatures.

3.5. Comparison with the reactions of the pyridine and pyrimidine radical cations

The results from the new reactions of acetylene with the benzonitrile, phenylacetylene, and styrene cations are consistent with our previous studies of the acetylene reactions with the benzene, phenyl, pyridine, and pyrimidine cations. Strong variation in reactivity is observed depending on the nature of the substituent group in the cation ring. For example, the reactions of acetylene with styrene and phenylacetylene cations appear to form one stable product ion but the reactions with the benzonitrile cation result in sequential products at room temperature. The measured rates indicate a reaction efficiency that varies from 2.8% at 304 K in the case of the acetylene reaction with the benzonitrile ion to the very low efficiency of 10^{-4} observed for the addition of acetylene onto the styrene cation at 588 K. These cations are clearly less reactive than pyridine and pyrimidine cations. For example, our previous studies indicate that the sequential reactions of acetylene with both the pyridinium and pyrimidinium ions result in exothermic addition/H-elimination channels leading to the formation of the bicyclic quinolizinium and pyrid [1] pyrimidinium cations as summarized in Scheme 1 below [26].

The mechanisms of the nitrogen incorporation in the PAH ions are important in understanding the ion chemistry in a nitrogen rich atmosphere such as that of Titan [9,13,58–61]. DFT calculations indicate that substitution of a carbon atom with nitrogen in the

benzene cation ring leads to lowering or eliminating the barrier to the acetylene addition [46–54]. These predictions are experimentally verified by the observation of fast sequential reactions of acetylene with the pyridine and pyrimidine cations [26]. The sequential reactions of acetylene with the benzonitrile cations studied in this work provide another mechanism for the incorporation of nitrogen in complex organic ions. The observed reactions could explain the possible formation of nitrogen-containing complex organics by gas phase ion–molecule reactions involving the pyridine, pyrimidine, and benzonitrile cations with acetylene under a wide range of temperatures and pressures in astrochemical environments such as the nitrogen-rich Titan's atmosphere [9,13,58–61].

3.6. Trends in reaction kinetics and structures of the product ions

In the present and pervious work, we observed covalent additions in the reactions of acetylene with six ionized aromatics and the phenyl cation as shown in Fig. 14 [25,26,38]. A very wide range of reaction rates has been found ranging from very slow reactions with energy barriers as in the case of benzene and styrene radical cations to reactions occurring at the collision rate as in the case of the pyrimidinium cation [26,38].

The high reactivity of acetylene towards the pyrimidinium ion is reflected in the measured rate coefficient of 1.0 ($\pm$1.2) $\times$ 10^{-9} cm^3 s^{-1} at 309 K which indicates a 100% reaction efficiency [26]. The rate coefficient measured for the acetylene reaction with the phenyl cation (generated from bromobenzene) is 7.1 ($\pm$1.4) $\times$ 10^{-10} cm^3 s^{-1}) indicating a reaction efficiency of nearly 50% at room temperature [25] and consistent with the value measured by SIFT (6.0×10^{-10} cm^3 s^{-1}) for the reaction of cyclic $C_6H_5^+$ with acetylene in 0.5 Torr He [62]. The measured rate coefficient of 1.4 ($\pm$1.2) $\times$ 10^{-10} cm^3 s^{-1} (at 304 K) for the acetylene reaction with the pyridinium ion indicates a reaction efficiency of nearly 10% which is significant for the production of large organic ions in the gas phase [26]. For the benzonitrile cation, the rate for the formation of the first ($C_9NH_7^{\bullet+}$) adduct with acetylene is 4.2 ($\pm$2.5) $\times$ 10^{-11} cm^3 s^{-1} with a reaction efficiency of 2.8% at 304 K. The acetylene reaction with the phenylacetylene cation is considered to be slow since it has only a reaction efficiency of 0.001 at room temperature. However, the acetylene reaction with the styrene radical cation was the slowest observed reaction with a rate coefficient of 1.3×10^{-13} cm^3 s^{-1} at 588 K comparable to the observed rate for the acetylene reaction with the benzene radical cation at 600 K [38].

The sequential addition/elimination reactions of acetylene with the benzene radical cation at high temperatures (500–600 K) can lead to the generation of naphthalene-type ions [38]. The high reactivity of the pyridinium ion towards acetylene at room temperature is in sharp contrast to the very low reaction efficiency (10^{-5}) observed for the addition of acetylene on the benzene cation [26,38]. This confirms that the barrier to the aromatic cation ring growth can be overcome by the substitution of a ring carbon atom (CH) with a nitrogen atom [44,45]. Thus, nitrogen-containing complex organics can be produced by the sequential reactions of acetylene with ionized heterocyclic aromatics such as the pyridinium and pyrimidinium ions. The phenylium ion also exhibits high reactivity towards acetylene leading to the formation of 2-phenyl-ethenylium ion ($C_8H_7^+$) with a reaction efficiency of nearly 50% at room temperature [25]. The high reactivity of the phenylium ion towards acetylene confirms that the first step in the cation ring growth mechanism is the loss of an aromatic H atom. The sequential addition of two acetylene molecules onto the benzonitrile cation could result in the formation of multiple cyclic structures which may react further with small molecules such as acetylene or hydrogen cyanide to form larger polycyclic ions. Although only one covalent adduct was observed in the acetylene reactions with the phenylacetylene cation at room temperature, the chemistry occurring at higher temperatures suggests an interesting polymerization process leading to the formation of higher naphthalene(acetylene)$_n$ adduct ions as well as polyacetylene polymer ions. Finally, the reactivity of acetylene towards the styrene radical cation appears to be very low and it results in the acetylene addition on both the $CHCH_2$ group as well as within the styrene ring which could lead to the formation of fused ring structures following the second addition of acetylene at higher temperatures.

4. Conclusions

In this work, we presented direct experimental evidence for the formation of covalently-bonded organic ions by gas phase reactions of acetylene with the benzonitrile, phenylacetylene, and styrene radical cations, and compared these results with the previously studied acetylene reactions with the benzene, phenyl, pyridine, and pyrimidine cations. In all cases, synthetic channels with increased numbers of carbon atoms are found in all the observed reactions. The resulting covalently-bonded precursor ions can undergo further growth to form polycyclic aromatic hydrocarbon ions including nitrogen-containing PAH ions. The observed chemistry under a wide range of experimental conditions, including extreme temperatures as high as 650 K, strongly implies a series of ion–molecule reactions that can lead from a simple molecule such as acetylene to polycyclic complex organic ions. The product ions resulting from the sequential reactions of acetylene can, in turn be neutralized by charge transfer or recombination, to produce large neutral PAHs. Therefore, ion–molecule reactions can contribute to the formation of higher hydrocarbons and PAHs in ionizing environments. The observed reactions could explain the possible formation of complex organics under a wide range of temperatures and pressures in astrochemical environments such as the nitrogen-rich Titan's atmosphere. The current results suggest searching for spectroscopic evidence for these organics in Titan's atmosphere.

Acknowledgments

We thank the National Science Foundation (CHE-0911146) and NASA (NNX08AI46G) for the support of this work.

Appendix A. Supplementary data

Supplementary data associated with this article can be found, in the online version, at http://dx.doi.org/10.1016/j.ijms.2014.08.023.

References

[1] K.-H. Homann, Angew. Chem. Int. Ed. 37 (1998) 2434–2451.
[2] M. Frenklach, Phys. Chem. Chem. Phys. 4 (2002) 2028–2037.
[3] T. Mendiara, M.P. Domene, A. Millera, R. Bilbao, M.U. Alzueta, J. Anal. Appl. Pyrolysis 74 (2005) 486–493.
[4] C. Jäger, F.H. Huisken, H. Mutschke, I.L. Jansa, Th. Henning, Astrophys. J. 696 (2009) 706–712.
[5] M. Kalberer, D. Paulsen, M. Sax, M. Steinbacher, J. Dommen, A.S.H. Prevot, R. Fisseha, E. Weingartner, V. Frankevich, R. Zenobi, U. Baltensperger, Science 303 (2004) 1659–1662.
[6] E. Herbst, E.F. van Dishoeck, Annu. Rev. Astron. Astrophys. 47 (2009) 427–480.
[7] M.L. Cable, S.M. Hoerst, R. Hodyss, P.M. Beauchamp, M.A. Smoth, P.A. Willis, Chem. Rev. 112 (2011) 1882.
[8] S.A. Sanford, J. Aleon, Science 314 (2006) 1720–1724.
[9] J.H. Waite Jr., Young, D.T. Cravens, T.E. Coates, A.J. Crary, F.J. Magee, B. Westlake, Science 316 (2007) 870–875.
[10] J. Cernicharo, M. Heras, A.G.G.M. Tielens, J.R. Pardo, F. Herpin, M. Guelin, L.B.F. M. Waters, Astrophys. J. 546 (2001) L123–L130.
[11] P.M. Woods, T.J. Millar, A.A. Zulstra, E. Herbst, Astrophys. J. 574 (2002) L167–L170.

[12] J.R. Pardo, J. Cernicharo, Astrophys. J. 654 (2007) 978–987.
[13] H.B. Niemann, S.K. Atreya, S.J. Bauer, Nature 438 (2005) 779–784.
[14] A.G.G.M. Tielens, Annu. Rev. Astron. Astrophys. 46 (2008) 289–337.
[15] Y.M. Rhee, T.J. Lee, M.S. Gudipati, L.J. Allamandola, M. Head-Gordon, Proc. Natl. Acad. Sci. U. S. A 104 (2007) 5274–5278.
[16] M.S. El-Shall, C. Marks, J. Phys. Chem. 95 (1991) 4932.
[17] D.K. Bohme, Chem. Rev. 92 (1992) 1487–1508.
[18] T. Tsukuda, T. Kondow, J. Am. Chem. Soc. 116 (1994) 9555.
[19] M. Meot-Ner (Mautner), L.W. Sieck, M.S. El-Shall, G.M. Daly, J. Am. Chem. Soc. 117 (1995) 7737.
[20] Zhong, L. Poth, Z. Shi, J.V. Ford, A.W. Castleman Jr., J. Phys. Chem. 101 (1997) 4203.
[21] S. Lee, N.G. Gotts, G. von Helden, M.T. Bowers, J. Phys. Chem. 101 (1997) 2096–2102.
[22] M.S. El-Shall, Acct. Chem. Res. 41 (2008) 783–792.
[23] M.S. El-Shall, Y.N. Ibrahim, E.H. Alsharaeh, M. Meot-Ner (Mautner), S.P. Watson, J. Am. Chem. Soc. 131 (2009) 10066–10076.
[24] D. Ascenzi, J. Aysina, P. Tosi, A. Maranza, G. Tonachini, J. Chem. Phys. 133 (2010) 184308–184317.
[25] A.R. Soliman, A.M. Hamid, P.O. Momoh, M.S. El-Shall, D. Taylor, L. Gallagher, S. A. Abrash, J. Phys. Chem. A 116 (2012) 8925–8933.
[26] A.R. Soliman, A.H. Hamid, I. Attah, P. Momoh, M.S. El-Shall, J. Am. Chem. Soc. 135 (2013) 155–166.
[27] P.O. Momoh, I.K. Attah, M.S. El-Shall, R.P.F. Kanters, J.M. Pinski, S.A. Abrash, J. Phys. Chem. A (2014) , doi:http://dx.doi.org/10.1021/jp5010488 (in press).
[28] Y.M. Ibrahim, E.H. Alsharaeh, M. Meot-Ner (Mautner), S. Scheiner, M.S. El-Shall, J. Am. Chem. Soc. 127 (2005) 7053–7064.
[29] A.M. Hamid, A.R. Soliman, M.S. El-Shall, J. Phys. Chem. A 117 (2013) 1069–1078.
[30] A.M. Hamid, P. Sharma, R. Hilal, S. Elroby, S.G. Aziz, A.O. Alyoubi, M.S. El-Shall, J. Chem. Phys. 139 (2013) 84304.
[31] Y. Ono, C.Y. Ng, J. Am. Chem. Soc. 104 (1982) 4752–4758.
[32] H. Shinohara, H. Sato, N.J. Washida, Phys. Chem. 94 (1990) 6718–6723.
[33] J.A. Booze, T. Baer, J. Chem. Phys. 98 (1993) 186–200.
[34] M.T. Coolbaugh, S.G. Whitney, G. Vaidyanathan, J.F. Garvey, J. Phys. Chem. 96 (1992) 9139–9144.
[35] V. Hrouda, M. Roeselova, T. Bally, Phys. Chem. A 101 (1997) 3925–3935.
[36] P.O. Momoh, S.A. Abrash, R. Mabourki, M.S. El-Shall, J. Am. Chem. Soc. 128 (2006) 12408–12409.
[37] P.O. Momoh, M.S. El-Shall, Chem. Phys. Lett. 436 (2007) 25–29.
[38] P.O. Momoh, A.R. Soliman, M. Meot-Ner (Mautner), A. Rica, M.S. El-Shall, J. Am. Chem. Soc. 130 (2008) 12848–12849.
[39] P.O. Momoh, A.M. Hamid, A.R. Soliman, S.A. Abrash, M.S. El-Shall, J. Phys. Chem. Lett. 2 (2011) 2412–2419.
[40] R.A. Relph, J.C. Bopp, J.R. Roscioli, M.J. Johnson, J. Chem. Phys. 131 (2009) 114305.
[41] P.O. Momoh, A.M. Hamid, S.A. Abrash, M.S. El-Shall, J. Chem. Phys. 134 (2011) 204315.
[42] T. Allen, M. Ricks, G.E. Douberly, M.A. Duncan, Astrophys. J. 702 (2009) 301–306.
[43] J. Aysina, A. Maranzana, G. Tonachini, P. Tosi, D. Ascenzi, Chem. Phys. 138 (2013) 204310.
[44] A. Ricca, C.W. Bauschlicher Jr., E.L.O. Bakes, Icarus 154 (2001) 516–521.
[45] A. Ricca, C.W. Baushlicher Jr., M. Rosi, Chem. Phys. Lett. 347 (2001) 473–480.
[46] C.W. Bauschlicher Jr., R. Ricca, M. Rosi, Chem. Phys. Lett. 355 (2002) 159–163.
[47] I.K. Attah, S.P. Platt, M. Meot-Ner, S.G. Aziz, A.O. Alyoubi, M.S. El-Shall, J. Chem. Phys. 140 (2014) 114313–114324.
[48] M.J. Frisch, et al., Gaussian 03, Revision C.02, Gaussian, Inc., Pittsburgh, PA, 2004.
[49] A.R. Soliman, A.M. Hamid, S.A. Abrash, M.S. El-Shall, Chem. Phys. Lett. 523 (2012) 25–33.
[50] S. Yamabe, T. Fukuda, S. Yamazaki, J. Phys. Chem. A 116 (2012) 1289.
[51] D. Lavorato, J. Terlouw, G. McGibbon, T. Dargel, W. Koch, H. Schwarz, Int. J. Mass Spectrom. 7 (1998) 179–180.
[52] D.K. Bohme, S. Wlodek, J.A. Zimmerman, J.R. Eyler, Inter. J. Mass. Spec. Ion Proc. 109 (1991) 31.
[53] C.S. McEnally, L.D. Pfefferle, Combust. Sci. Technol. 128 (1997) 257.
[54] W.J. van der Hart, Int. J. Mass Spectrom. 214 (2002) 269.
[55] Y.A. Dyakov, C.K. Ni, S.H. Lin, Y.T. Lee, A.M. Mebel, Phys. Chem. Chem. Phys. 8 (2006) 1404.
[56] K. Schroeter, D. Schroder, H. Schwarz, J. Phys. Chem. A 103 (1999) 4174.
[57] C.L. Wilkins, M.L. Gross, J. Am. Chem. Soc. 93 (1971) 895.
[58] A.J. Coates, Philos. Trans. R. Soc. A 367 (2009) 773–788.
[59] N. Balucani, Chem. Soc. Rev. 41 (2012) 5473–5483.
[60] S. Pizzarello, W. Holmes, Geochim. Cosmochim. Acta 73 (2009) 2150–2162.
[61] M.L. Delitsky, C.P. McKay, Icarus 207 (2010) 477–484.
[62] V.G. Anicich, P.F. Wilson, M.J. McEwan, J. Am. Soc. Mass Spectrom. 14 (2003) 900–915.